

# A Survey of Optical Knots in Kepler's SNR

R. BANDIERA, *Osservatorio Astrofisico di Arcetri, Firenze, Italy*

S. VAN DEN BERGH, *Dominion Astrophysical Observatory, Victoria, Canada*

## 1. Introduction

Kepler's supernova remnant (SNR) is an ideal object for a direct investigation of the interaction of a blast wave with a highly inhomogeneous medium. Most of the optical emission comes from dense ( $n \sim 10^3 - 10^4 \text{ cm}^{-3}$ ) and compact ( $r \sim 10^{16} - 10^{17} \text{ cm}$ ) knots recently hit by the main shock. The physics of the interaction is complex and involves the formation of secondary shocks, cloud crushing and evaporation by saturated conduction (see McKee, 1988 for a review).

We here present some results of a long-term project on Kepler's SNR, directed towards the study of links between the kinematical, morphological and spectroscopical properties of a knot, and the phase of its interaction with the supernova blast wave. Kepler's SNR is a very young object (less than 400 yr old), and contains features that evolve with time-scales considerably shorter than a human lifetime. For this reason it represents one of those rare cases in which the evolution can be followed "in real time".

## 2. Morphology

After Kepler's supernova (SN 1604) faded away, more than three centuries passed before its remnant was discovered. In 1941 Baade (1943) first detected some nebulosity near the supernova position that was deduced from the historical records. He described Kepler's SNR as "a broken mass of bright knots and filaments covering a fan-shaped area", but actually detected only the N-W brightest part of the optical remnant.

In fact the location of this remnant is far from ideal for optical observations. It is highly reddened, and very crowded by field stars. Therefore faint filaments may be overwhelmed by the background, while some optical knots can be mistaken for stars. Deeper images of the nebular emission can be obtained only after a careful subtraction of the stellar continuum from narrow-band frames centred on conspicuous emission lines, like  $H\alpha + [N \text{ II}]$  (D'Odorico et al., 1986), but also  $[S \text{ II}]$ ,  $[O \text{ I}]$  or  $[O \text{ III}]$  (Blair, Long and Vancura 1991).

Such images reveal a great deal of structure. In addition to the brightest complex located on the N-W side of the remnant, there are some clumps of knots lying along the edge of the rem-

nant, and spanning directions from N-E to West (clockwise). Other groups of knots are located closer to the remnant centre. Fainter diffuse emission is also present along most of the northern rim of this SNR, as well as in the surroundings of the central groups of knots. No optical emission can be detected along the southern rim of the remnant.

Actually the optical images are not the most suitable for defining centre and size of Kepler's SNR; but one could use radio and X-ray images (Matsui et al., 1984), where the remnant looks pretty circular. However also at these wavelengths it shows a strong asymmetry in the emission, with a N-W limb considerably brighter than the rest of the remnant.

## 3. Kinematics – A Bow Shock Model?

By a comparison of plates covering the period 1942–1976, van den Bergh and Kamper (1977) were able to measure proper motions for 19 knots. Furthermore they collected radial velocity measurements for a few knots.

Their data were consistent with an "expansion age" of less than  $2 \times 10^4$  yr. Therefore it became clear that the optical knots in Kepler's SNR have not been ejected by the supernova. On the other hand they are too dense and clumped to be interstellar (recall that the remnant is located about 500 pc above the Galactic plane, for a distance of 4.5 kpc). Very likely the optical knots originated from a wind of the stellar progenitor. This hypothesis is also supported by the presence of a slight nitrogen overabundance (Dennefeld, 1982; Leibowitz and Danziger, 1983). In some respects the knots resemble the "Quasi Stationary Flocculi" in Cassiopeia A.

Knot velocities, typically only some hundred km/s, can be interpreted as random motions added to a common translation, pointing towards the N-W. Bandiera (1987) noticed that such a translation points to the direction where the remnant is brightest, in the optical as well as in radio and X rays, and explained this in the following way:

Assuming that this material originated from a stellar wind, its common motion may reflect the motion of the supernova progenitor. During that mass-loss phase, the wind was interacting with the interstellar medium, and formed a bow

shock in the direction of the stellar motion. In the bow shock the gas was compressed, allowing the condensation of dense clumps. Now the supernova blast wave moves through this dense and inhomogeneous medium. The effect of this is an enhanced emission in radio and X rays on that side. When the most compact clumps are "ignited" by the arrival of the blast wave they become visible as optically emitting knots.

Since the time-scale for the evolution of knots is considerably shorter than the remnant age, the optical knots trace the actual position of the supernova blast wave. Knots are visible only on an annulus at the intersection of the bow shock with the blast wave. Since the common translation also has a radial component, the bow shock geometry is seen from an oblique perspective, and this annulus appears as an ellipse. On this hypothesis the knots projected near the central regions of the SNR are actually part of this (distorted) ellipse. With the expansion of the blast wave, new knots will appear on an ellipse that increases in size and shifts in position as well.

This geometry allows one to predict where new knots will appear. A non-trivial prediction concerns the central knots. These new knots should brighten to the south of those already existing (Bandiera 1988).

## 4. The Restoration of Old Plates

Here we shall describe the most important phases of a work (Bandiera and van den Bergh, 1991a), that allowed us to obtain cleaner and deeper images, and to follow in detail the motions of many knots and the evolution of their intensities over the last half century.

We used plates taken with the Hooker 2.5-m reflector (1941–1943) and with the Hale 5-m telescope (1950–1983). As already mentioned in Section 2, the nebular emission is immersed in a crowded stellar field. This is particularly evident on old plates, exposed with broad-band filters. As a first step, we decided to "restore" these plates, by subtraction of the stellar continuum, with the aim of also extracting from them information that was originally hidden. This requires an off-line reference image for the subtraction. However we did not expect the stellar field to have experienced significant changes

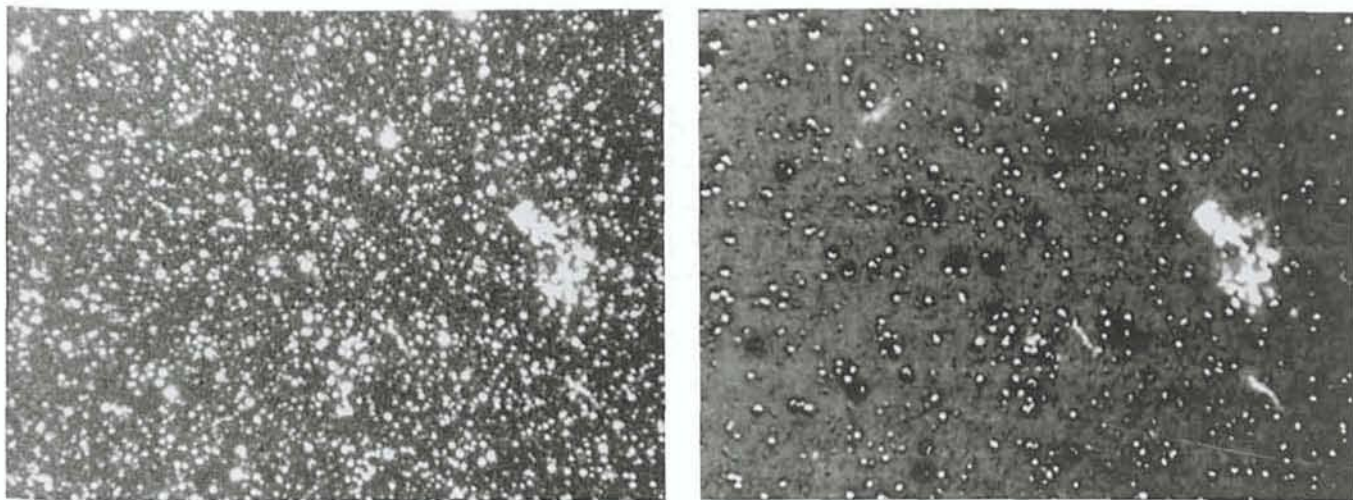


Figure 1: (a) good-quality photographic plate of Kepler's SNR (Hale 5-m telescope, May 1950); (b) the same after restoration by subtraction of the stellar continuum.

over the last decades. We therefore decided to use an image taken recently.

Observations were carried out in 1989 with the 1.5-m Danish telescope on La Silla, with the RCA CCD No. 15, using broad-band as well as interference filters centred on  $H\alpha+[N II]$ ,  $[S II]$  lines, and on the nearby continuum. Our aim was to produce a reference image for the stellar field with a spectral response similar to that of the old plates. In this respect a Bessell R filter was found to give the best results. We first obtained  $H\alpha+[N II]$  and  $[S II]$  images of the nebular emission, by subtracting the stellar continuum, after a proper alignment of the frames and an approximate equalization of the point spread functions. They were then used for subtracting the nebular component from the frame with the Bessell R filter. In all the steps of the reduction procedure we stressed the production of images that were as clean as possible, while deemphasizing the detection of very faint structures.

The next step was the subtraction of the stellar continuum from the old plates. This stellar subtraction can be carried out only after a linearization of the characteristic curve of the photographic plates. Since this was unknown, we had to derive it from the plate itself, by comparison with the (linear) CCD frame. This is a difficult task, mainly because the point spread functions of the two images are also different. We solved the problem in an approximate way by comparing the intensities of a set of stars selected independently on the plate and on the CCD reference frame, using the INVENTORY routine, implemented in MIDAS. By this procedure the image of the bright stars cannot be completely removed. However, for fainter stars which are more numerous, the characteristic curve of the plate can be fitted with greater accu-

racy, resulting in a more efficient stellar subtraction. As an example, Figure 1a shows the appearance of a photographic image of Kepler's SNR, obtained in 1950 with a broad-band red filter. Figure 1b shows the same image, after the stellar subtraction procedure described above.

## 5. A Catalogue of Optical Knots

After "cleaning" the old plates from stellar contamination, following the evolution of the nebular emission becomes an easier task. The complete set of restored images has been published by Bandiera and van den Bergh (1991a). Some knots are seen to brighten considerably. Most of these lie on the external part of the northern rim, but some are also located in the central regions of the remnant. The evolution of knots is of particular interest for the understanding of the geometry of this object. Newer knots brightened to the south of those already existing; in qualitative agreement with the predictions of the bow shock model (Bandiera and van den Bergh, 1991b) described in Section 3.

The quality of the images is good enough to also allow a quantitative analysis of the evolution of the optical remnant. As a first step, a catalogue of emitting knots has been prepared. In Kepler's SNR optical knots usually look to be well defined. When filamentary structures are present, they usually consist of a group of aligned knots. In order to avoid selection effects produced by manual recognition and centring of knots, we preferred to perform an automatic search (by INVENTORY) in the region where knots are present. Furthermore, this search was performed independently on the different plates. We retained as real only those knots that were detected independently on most of

the plates. On average a knot was detected on 9 of the 12 available frames. Our catalogue was not intended to be complete. Even a few rather bright knots were discarded because they were almost coincident with a poorly subtracted star. Furthermore, a few very recent knots were not included, because they were only present on a few images. Our catalogue lists only knots whose parameters can be determined with some accuracy. The total number of knots in our catalogue is 50 compared to the 19 knots catalogued by van den Bergh and Kamper (1977), who used a similar set of plates.

INVENTORY gives both positions and intensities of sources. These positions can be used to determine astrometric motions of individual knots. Proper motions are combined to measure the amount of common translation, as well as expansion velocity. After correcting for Galactic rotation the components of the average knots motion are  $117 \pm 10$  km/s and  $105 \pm 11$  km/s, toward West and North, respectively; the expansion velocity is instead  $67 \pm 26$  km/s (for a distance of 4.5 kpc). These values are consistent with those of van den Bergh and Kamper (1977), but have a much higher accuracy.

Approximate photometry has been obtained by comparing the intensities of corresponding knots in different images, after additional corrections for effects of the residual non-linearity in the restored images. Absolute calibration is provided by the knot fluxes given by D'Odorico et al. (1986). At the end of this reduction we obtained light curves (basically in  $H\alpha+[N II]$  emission) for all catalogued knots over a period of 40–50 yr. The relative accuracy on the intensity estimates is about 30%.

Bandiera and van den Bergh (1991a) present all available quantitative infor-

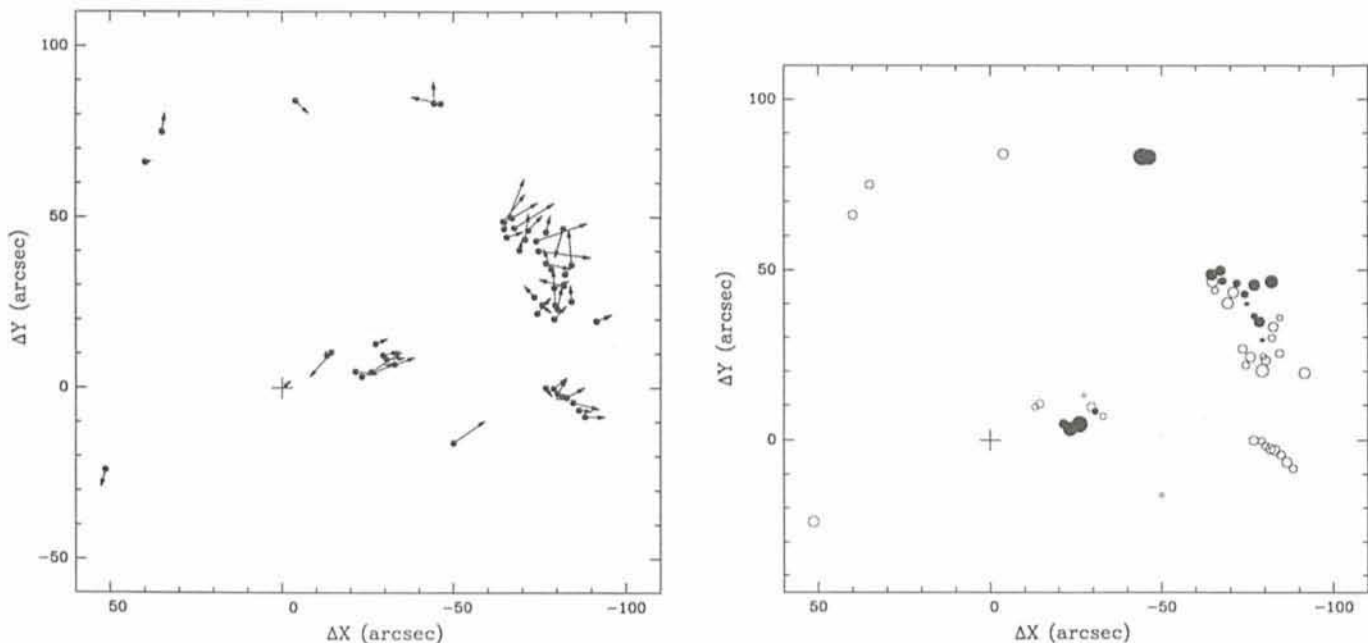


Figure 2: Mapping (a) of proper motions and (b) of evolution in brightness of catalogued knots in Kepler's SNR (see text).

mation derived from astrometry and photometry of the catalogued knots. Our Figures 2a and 2b give a synoptic picture of the proper motions of knots and of their evolution in brightness, respectively. In Figure 2a each arrow represents the proper motion of a knot over 400 yr (the present SNR age). The cross indicates the position of the centre of the radio and X-ray image, and the arrow from its centre indicates the common translation of the pattern of knots. In Figure 2b a circle centred at the position of each catalogued knot represents its evolutionary phase: filled circles indicate brightening (newer knots), while open circles indicate fading (older

knots). Larger circles indicate faster evolution. As already discussed above, newer knots brightened on the northern rim central regions of Kepler's SNR. Most knots are fading, with time-scales generally longer than those of the brightening ones (e-fold time-scales are up to 10 yr for brightening, and up to 30 yr for fading).

## 6. Effects of the Evolution on the Knots' Properties

Purpose of this Section is to give the reader a qualitative feeling of how the properties of knots depend on the phase of their evolution. Here we shall

present preliminary results based on images obtained with SUSI at the New Technology Telescope (May 1991), using narrow-band filters centred on  $H\alpha+[NII]$ ,  $[SII]$  and  $[OIII]$  lines, respectively. For each of these three filters, after the subtraction of the stellar continuum, the relative intensities of knots catalogued by Bandiera and van den Bergh (1991a) have been measured.

In Figures 3a and 3b knot intensities in different lines are plotted ( $[SII]$  vs.  $H\alpha+[NII]$ , and  $[OIII]$  vs.  $[SII]$ , respectively). Each knot is represented by a circle, whose characteristics indicate the evolutive phase of that knot, according to the conventions already used in Fig-

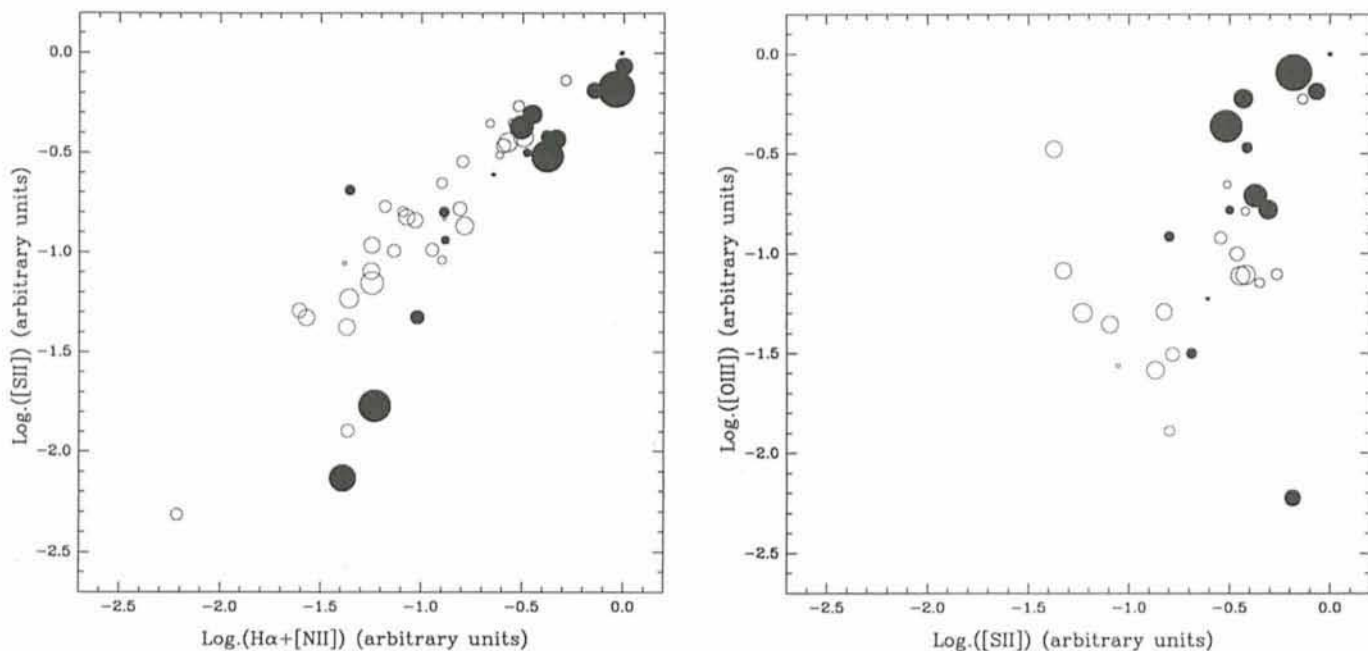


Figure 3: Distribution of knots at different evolutionary phases in the (a)  $(H\alpha+[N II]) - [S II]$  and (b)  $[S II] - [O III]$  intensity-planes (see text).

ure 2b. Figure 3b contains only 30 knots, because the INVENTORY routine failed to detect [O III] emission from the others.

From both figures it is seen that the regions containing younger knots (filled circles) are separated from those containing older knots (open circles). In Figure 3a the correlation between [S II] and  $H\alpha + [N II]$  intensities is rather good, but older knots are typically brighter in [S II]. However, in Figure 3b this correlation is poor. Most of the brighter knots in [O III] are young, while this is not so for [S II].

These results qualitatively agree with a scenario in which the knots are initially at a higher ionization level, which then decreases with time. However, quantitative conclusions are beyond the scope of this discussion which is still based on incomplete data.

## 7. What's Next?

We have shown that a spectroscopic survey of optical knots, if combined with the present knowledge on their evolution, can provide a wealth of information on the temporal behaviour of the interaction of a blast wave with dense and compact clumps. Therefore, it might represent a useful benchmark for theoretical models of this interaction. The next step in this programme is to obtain a complete set of spectra for all catalogued knots. Intensity information on many lines would allow one to see how physical quantities, like densities and temperatures, evolve with time. A further goal is to discriminate those spectral features that mostly depend on evolutionary phase from those directly related to the intrinsic properties of a knot, like original density, size, etc. . . .

A detailed mapping of the radial velocities of knots is also planned. With Kepler's SNR we are at present in the paradoxical situation that proper motions are known in more detail than radial velocities. These two components, once combined, will give a 3-dimensional picture of the kinematics of this object. Such a study could provide valuable information on the structure and possibly also on the nature of this remnant.

The present advanced stage of our investigation is mostly due to observations taken at La Silla. The equipment present at La Silla is particularly suitable for a completion of the survey with a reasonably short observing time. Multi-Object-Spectroscopy facilities are the most suitable for optimizing observing time when spectra are needed for a large number of nearby objects. A private instrument (but well integrated in La Silla environment) like CIGALE Fabry-Perot scanning interferometer from

Marseille Observatory (Boulesteix et al., 1984), however, is ideal for radial velocity mapping.

## References

- Baade, W. 1943, *Ap.J.*, **97**, 119.  
 Bandiera, R. 1987, *Ap.J.*, **319**, 885.  
 Bandiera, R. 1988, In *Supernova shells and their birth events*, ed. W. Kundt, Lecture Notes in Physics Series, Springer Verlag, Berlin, p. 81.  
 Bandiera, R., van den Bergh, S. 1991a, *Ap.J.*, **374**, 186.  
 Bandiera, R., van den Bergh, S. 1991b, In *SN 1987A and other Supernovae*, Proceedings of ESO/EIPC Workshop, eds. I.J. Danziger and K. Kj ar, p. 661.

- Blair, W.P., Long, K.S., Vancura, O. 1991, *Ap.J.*, **366**, 484.  
 Boulesteix, J., Georgelin, Y.P., Marcelin, M., Monnet, G., 1984, In *Instrumentation in Astronomy*, Proc. SPIE 445, eds. V.A. Boksenberg, and D.L. Crawford, p. 37.  
 Dennefeld, M. 1982, *Astron. Astrophys.* **112**, 215.  
 D'Odorico, S., Bandiera, R., Danziger, J., Focardi, P. 1986, *Astr. J.*, **91**, 1382.  
 Leibowitz, E.M., Danziger, I.J. 1983, *M.N.R.A.S.*, **204**, 273.  
 Matsui, Y., Long, K.S., Dickel, J.R., Greisen, E.W. 1984, *Ap. J.*, **287**, 295.  
 McKee, C. 1988. In *Supernova Remnants and the Interstellar Medium*, IAU Coll. 101, eds. R.S. Roger, and T.L. Landecker, Cambridge Univ. Press, New York, p. 205.  
 van den Bergh, S. Kamper, K.W. 1977, *Ap. J.*, **218**, 617.

## Subarcsecond Structures in Kepler's SNR

Narrow-band frames of Kepler's SNR have been obtained on May 15, 1991, using SUSI at the New Technology Telescope, during an official run devoted to imaging and spectroscopy of this object. Here we present images of the most conspicuous clusters of optical knots. These images are based on a 10-min exposure frame, taken with a narrow-band filter centred on  $H\alpha + [N II]$  lines; the seeing was 0.7 arcsec.

After standard reduction, the stellar continuum has been subtracted using another 10-min exposure with an off-line narrow-band filter, obtained in similar seeing conditions. Before stellar subtraction the two point-spread functions have been carefully equalized, taking care of degrading the resolution as little

as possible. In the resulting image the residuals are about 7% (peak-to-peak) of the original stellar images, while the seeing has been degraded to 0.8 arcsec.

In order to extract details on the fine structure of the optical knots, we digitally simulated an unsharp-masking procedure. We convolved the image with a gaussian function of 1.8 arcsec FWHM, and added a constant value of 1.5 times the sky background. We finally divided the original image by this "mask". The effect of such a procedure is that of depressing the diffuse emission, as well as that of compressing the dynamical range. The dynamical compression allows us to see at the same time knots that originally were differing in intensity even by a factor 100. The results are

